

Lecture 5

Ion Implantation

Reading:

Chapter 5

Ion Implantation

Shockley patented the concept of Ion Implantation for semiconductor doping in 1956 (2 years after Pfann patented the diffusion concept). First commercial implanters were introduced in 1973. Modern implanters are multi-million dollar machines!

Concept:

Ions (charged atoms or molecules) are created via an enormous electric field stripping away an electron. These ions are filtered and accelerated toward a target wafer, where they are buried in the wafer. The depth of the implantation depends on the acceleration energy (voltage). The dose is very carefully controlled by integrating the measured ion current. This integration process tends to minimize noise in the measurement of the ion current, resulting in several decimal places of accuracy in the dose

$$Q_T = \frac{1}{q \text{ Area}} \int I dt$$

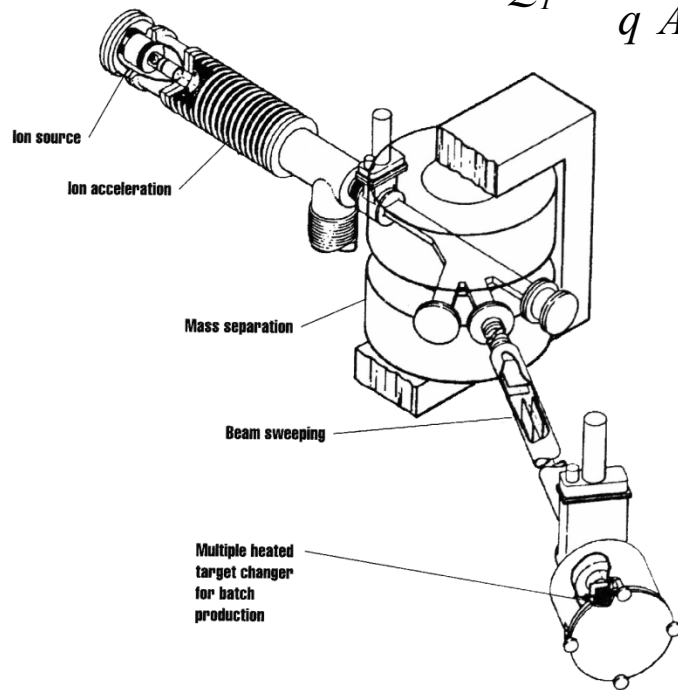


Figure 5-1 Schematic of an ion implanter (after Mayer et al., reprinted by permission, Academic Press).

Ion Implantation

Advantages of Ion Implantation:

- 1.) Very precise control of the dose
- 2.) Independent control of impurity depth and dose
- 3.) Very fast (1 12" wafer can take as little as 25 seconds for a moderate dose)
- 4.) Can perform retrograde profiles that peak at points inside the wafer (as opposed to the wafer surface). Draw an example
- 5.) Complex profiles can be achieved by multi-energy implants.

Disadvantages of Ion Implantation:

- 1.) Very deep and very shallow profiles are difficult
- 2.) Not all the damage can be corrected by post-implant annealing.
- 3.) Typically has higher impurity content than does diffusion.
- 4.) Often uses extremely toxic gas sources such as arsine (AsH_3), and phosphine (PH_3).
- 5.) Expensive

Applications:

Doping, SIMOX, H and He isolation in GaAs, and Smart cut technologies

Ion Implantation

Ions are imbedded into the wafer and are scattered at random angles. The ions lose kinetic energy, thus, slowing to a stop, by 2 mechanisms:

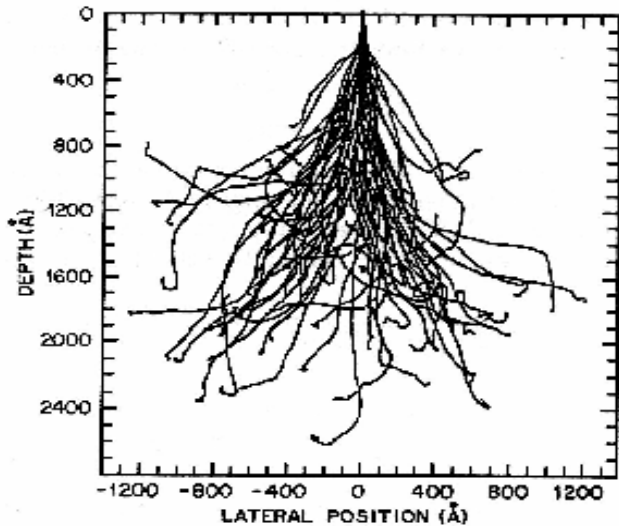
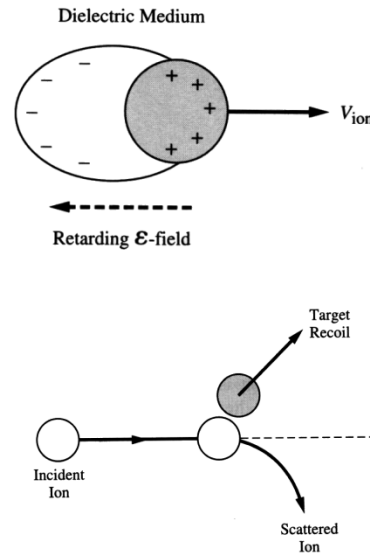


FIGURE 1
Monte Carlo calculation of 128 ion tracks for 50 keV boron implanted into silicon.



Electronic: Electric field “drag” created by positive ion moving in a flood of electrons

Nuclear: Impact with cores of atoms causes damage.

- 1.) Nuclear collisions: ions collide with atoms. The positively charged ions are coulombically repelled by the positive cores of the wafers lattice atoms. This coulombic repulsion is “screened” by the cloud of electrons surrounding each atom.
- 2.) Electronic stopping: If ions graze the lattice atoms, they do not interact with the lattice atom’s electrons and not the positive core. This interaction slows the ions by “viscous friction” similar to a rock thrown into water. Note: many electrons are freed from the lattice atoms creating an “ocean of electrons” that the ions must pass through.

The stopping power, S = energy loss per unit length of the ion path is ,

$$S = \left(\frac{dE}{dx} \right)_{nuclear} + \left(\frac{dE}{dx} \right)_{electronic} = S_n + S_e$$

Ion Implantation

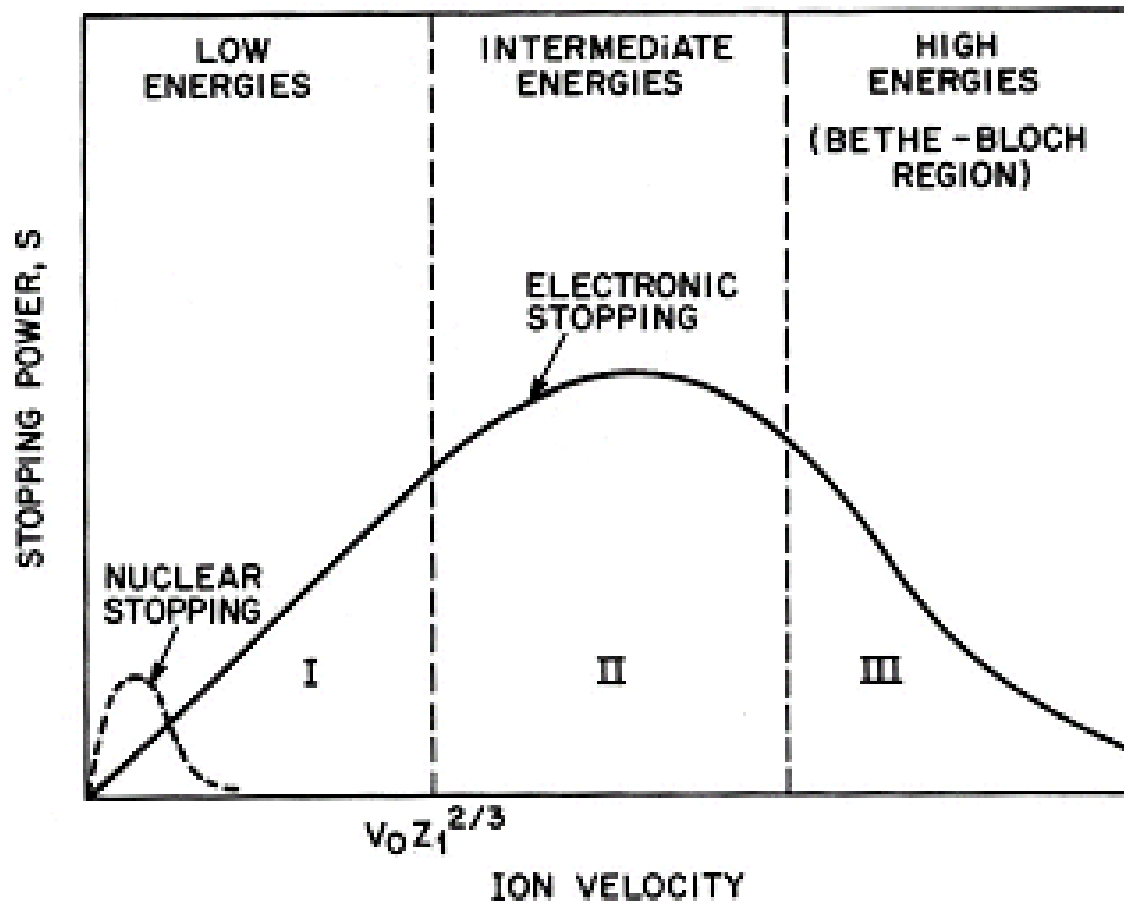


FIGURE 2

Nuclear and electronic components of the ion stopping power as a function of ion velocity. The quantity v_0 is the Bohr velocity, $q^2/4\pi\epsilon_0\hbar$, and Z_1 is the ion atomic number. (After Cruz, Ref. 6.)

Ion Implantation

Nuclear stopping is more important at lower atomic number (lighter elements) and lower ion velocities (low acceleration energy/voltage).

Electronic stopping dominates at higher atomic number (heavier elements) and higher ion energies.

The nuclear stopping power is complex to derive, not very accurate. Suggest you use Monte Carlo approaches like the software program “TRIM” instead.

The electronic stopping power can be approximated as:

$$S_e = \left(\frac{Z_1^{7/6} Z_2}{(Z_1^{2/36} + Z_2^{2/3})^{3/2}} \right) 4a_0 N v$$

where Z_1 is the ion atomic number, Z_2 is the lattice atom atomic number, a_0 is the Bohr radius (constant), N is the wafer atomic density, and v is the ion velocity.

Unit describes the energy loss (roughly) per plane of atoms passed. Thus, typically many thousands of atomic planes are traversed before the implanted atom comes to rest.

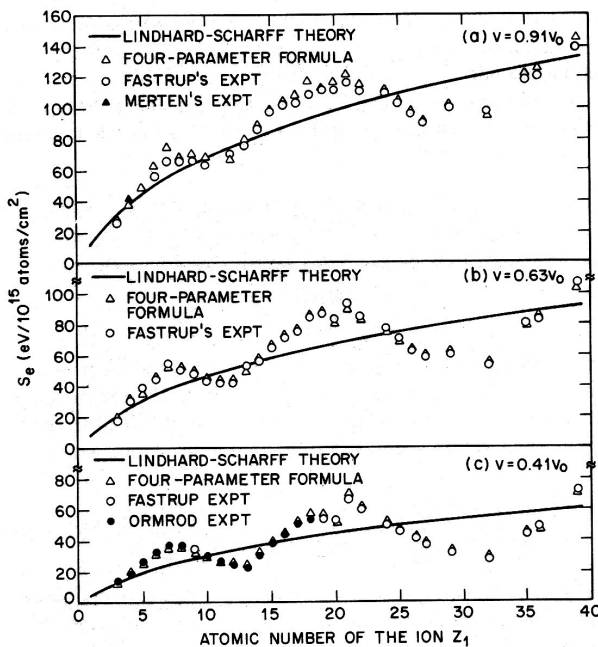


FIGURE 4
Electronic stopping powers for various ions in carbon, comparing theory with experiment. (After Xia and Tan, Ref. 9.)

Ion Implantation

Impurity Profiles

There are 2 popular descriptions of the implanted profile:

1.) Simple Gaussian

The simplest approximation to an Ion implanted profile is a Gaussian distribution.

$$n(x) = n_o e^{\left(\frac{-(x-R_p)^2}{2\sigma_p^2}\right)} \quad \text{where } n_o = \frac{Q_T}{\sigma_p \sqrt{2\pi}}$$

R_p is the “projected range” of the ion

σ_p (ΔR_p) is the straggle.

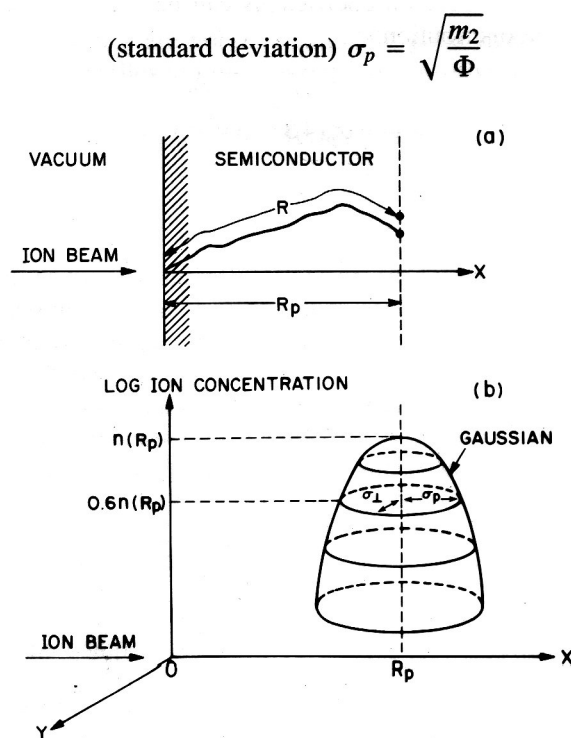


FIGURE 5

Schematic views of the ion range. (a) The total path length R is longer than the projected range R_p . (b) The stopped atom distribution is two-dimensional Gaussian. (After Sze, Ref. 10.)

Ion Implantation

This approximation to the profile is good for lower energies but is less correct of higher energies where the profile is “skewed”.

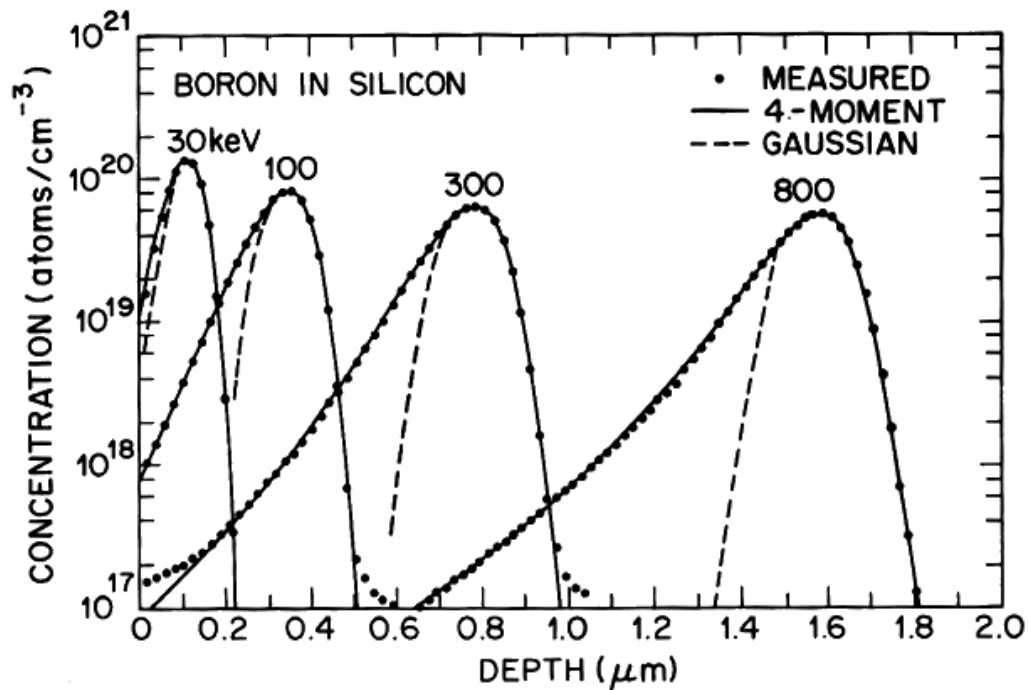


FIGURE 6

Boron implanted atom distributions, comparing measured data points with four-moment (Pearson IV) and Gaussian fitted distributions. The boron was implanted into amorphous silicon without annealing. (After Hofker et al., Ref. 11.)

- 1.) [Negative skewness](#) (shown above) means the distribution is shifted toward the surface, possibly due to back scattering: Common for light elements at high energy
- 2.) [Positive skewness](#) means the distribution is shifted away from the surface, possibly due to channeling (will discuss shortly): Common for heavy elements at low energy

Ion Implantation

2.) Moments Description:

When a profile deviates from the ideal Gaussian, we can describe it by its **five** moments taken about R_p ,

$$m_i = \int_{-\infty}^{+\infty} (x - R_p)^i n(x) dx$$

0th moment: Dose

(Q_T)
$$Q_T = m_0 = \int_{-\infty}^{+\infty} n(x) dx$$

1st Moment: Range (R_p) (= average depth from the surface)

$$m_1 = Q_T R_p = \int_{-\infty}^{+\infty} x n(x) dx$$

2nd Moment: standard deviation (or straggle, σ_p) (Half width at half maximum of a simple Gaussian)

$$m_2 = Q_T \sigma_p^2 = \int_{-\infty}^{+\infty} (x - R_p)^2 n(x) dx$$

3rd Moment: Skewness (γ) (measure of the profiles tendency to lean toward or away from the surface)

$$m_3 = \gamma Q_T \sigma_p^3 = \int_{-\infty}^{+\infty} (x - R_p)^3 n(x) dx$$

4th Moment: kurtosis (β) (measure of flatness: A perfect Gaussian has a kurtosis of 3. Larger kurtosis means the profile is flatter near its peak).

$$m_4 = \beta Q_T \sigma_p^4 = \int_{-\infty}^{+\infty} (x - R_p)^4 n(x) dx$$

Ion Implantation

When the kurtosis is not known, it can be approximated by, $\beta \sim 2.8 + 2.4\gamma^2$

These characteristics can be used to generate profiles using the Pearson family of distributions defined by solutions to the equation,

$$\frac{df(s)}{ds} = \frac{(s - b_1)f(s)}{b_0 + b_1s + B_2s^2}$$

where $s = x - R_p$ and,

$$A = 10\beta - 12\gamma^2 - 18$$

$$b_0 = -\sigma_p^2 \frac{(4\beta - 3\gamma^2)}{A}$$

$$b_1 = -\gamma\sigma_p \frac{(\beta + 3)}{A}$$

$$b_2 = \frac{-(2\beta - 3\gamma^2 - 6)}{A}$$

Ion Implantation

There are seven different solutions to the Pearson equation. For ion implantation, the Pearson IV solution is used,

$$f(s) = f(x = R_p) e^{\left(\frac{1}{2b_2} \ln(b_0 + b_1s + b_2s^2) - \frac{\frac{b_1}{b_2} + 2b_1}{\sqrt{4b_0b_2 - b_1^2}} \tan^{-1} \left(\frac{2b_2s + b_1}{\sqrt{4b_0b_2 - b_1^2}} \right) \right)}$$

This function has a peak at $x=R_p+b_1$ and is valid when the coefficients satisfy:

$$0 < \frac{b_1^2}{4b_0b_2} < 1$$

For concentrations, $f(s)=n(x)$ and $f(x=R_p)=n(x=R_p)$

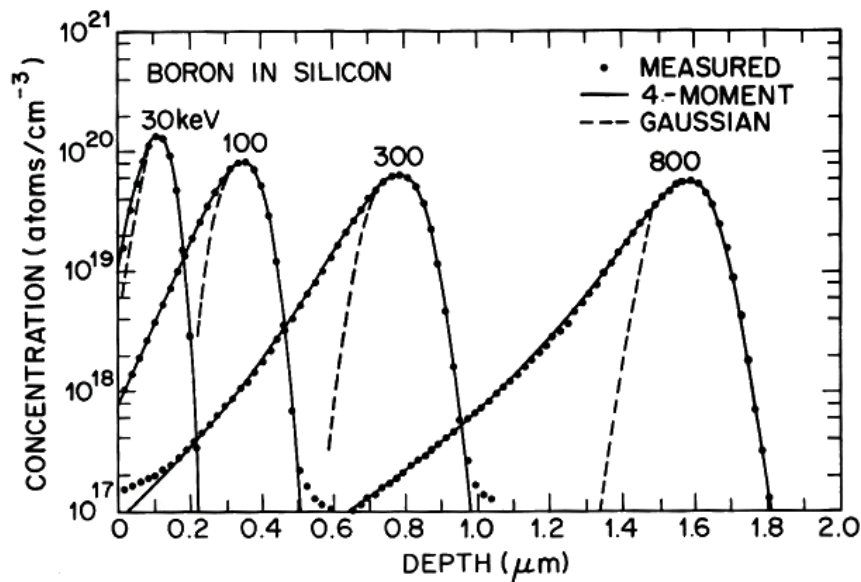


FIGURE 6
Boron implanted atom distributions, comparing measured data points with four-moment (Pearson IV) and Gaussian fitted distributions. The boron was implanted into amorphous silicon without annealing. (After Hofker et al., Ref. 11.)

Ion Implantation

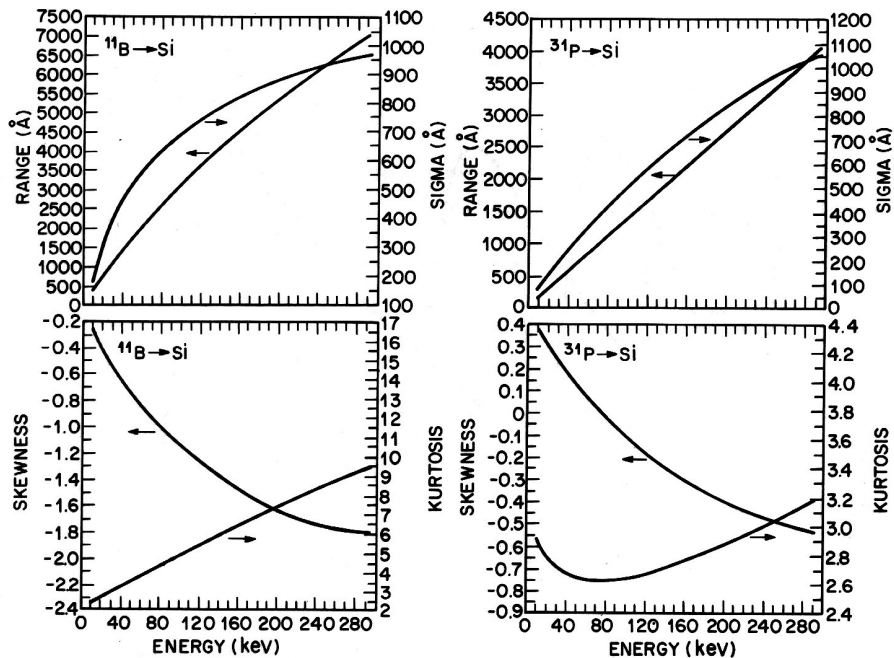


FIGURE 7
 Monte Carlo – calculated moments of implanted atom distributions for common dopants in silicon.
 (After Petersen, Fichtner, and Grosse, Ref. 12.)

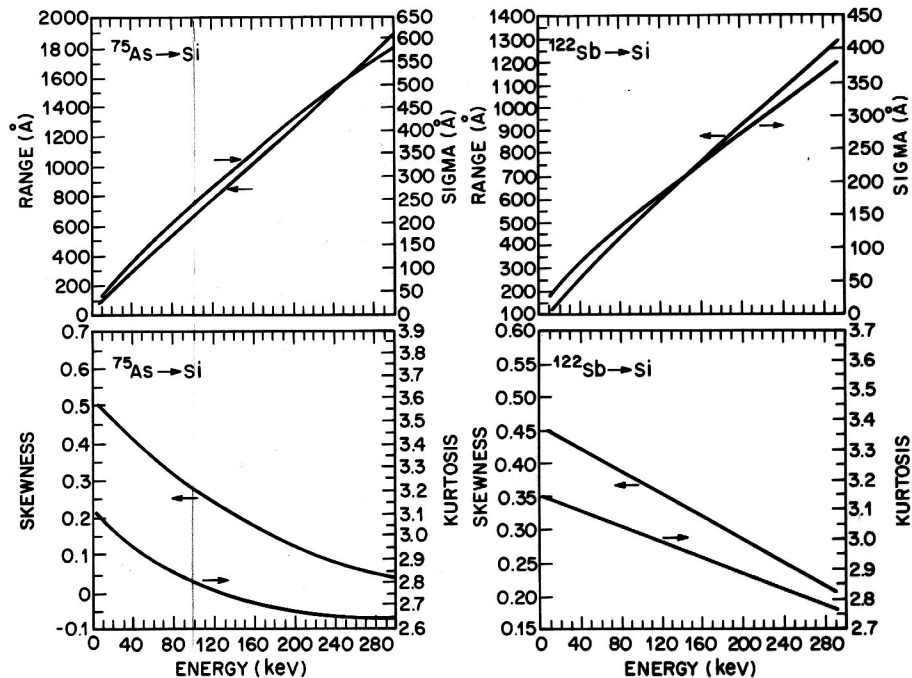


FIGURE 7 (CONTINUED)

Ion Implantation

Masking

Thick or dense materials can be used to “protect” regions from being implanted. The choice of materials determines the “Stopping Power” of the mask. Denser materials are more effective.

TABLE 1
Boron ranges in various materials^{13,14,15}

100 keV boron implantation				
Material	Symbol	Density (g/cm ³)	$R_p(\text{\AA})$	$\sigma_p(\text{\AA})$
Silicon	Si	2.33	2968	735
Silicon dioxide	SiO ₂	2.23	3068	666
Silicon nitride	Si ₃ N ₄	3.45	1883	408
Photoresist AZ111	C ₈ H ₁₂ O	1.37	10569	1202
Titanium	Ti	4.52	2546	951
Titanium silicide	TiSi ₂	4.04	2154	563
Tungsten	W	19.3	824	618
Tungsten silicide	WSi ₂	9.86	1440	555

Masks can also be used to create “Shallow Implants”:

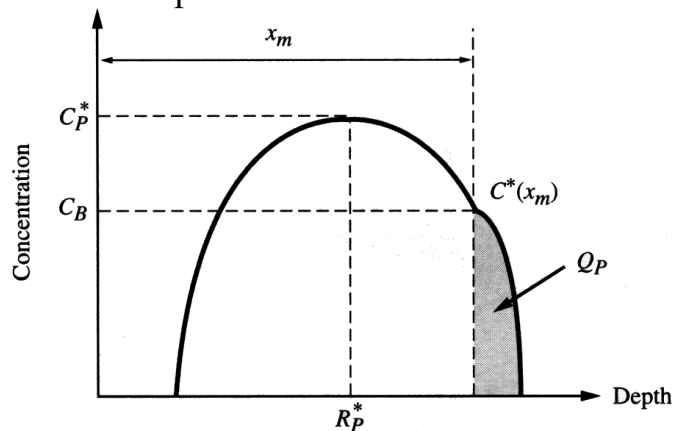


Figure 8-5 Schematic of a masking process, where a dose Q_p penetrates the mask of thickness x_m .

Ion Implantation

Diffusion During Subsequent Anneals

During high temperature steps after implant (most commonly an activation anneal), the implanted impurities will begin to diffuse, broadening the implantation profile.

For implantations far away from the surface and for reasonable short characteristic diffusion lengths, the new profile can be approximated by:

$$n(x) = \frac{Q_T}{\sqrt{\sigma_p^2 + 2Dt} \sqrt{2\pi}} e^{\left(\frac{-(x-R_p)^2}{2(\sigma_p^2 + 2Dt)} \right)}$$

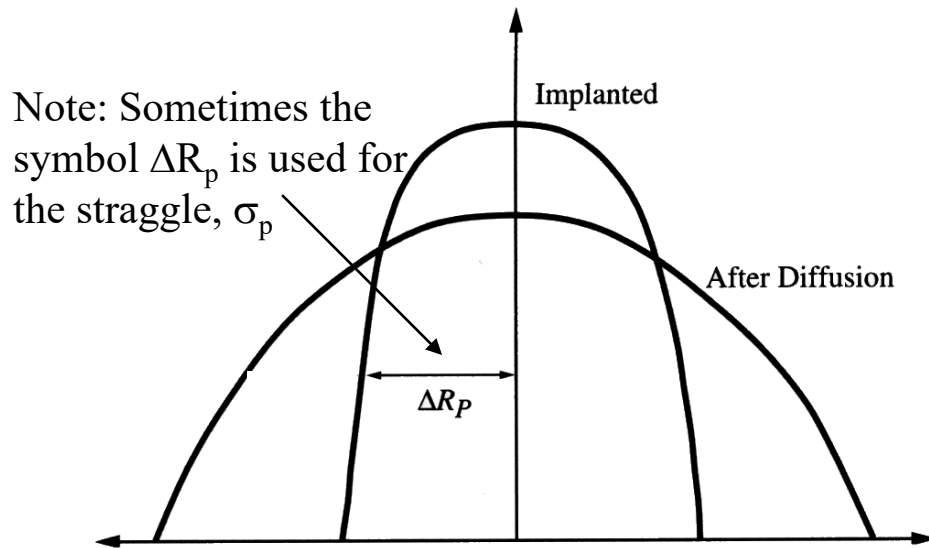


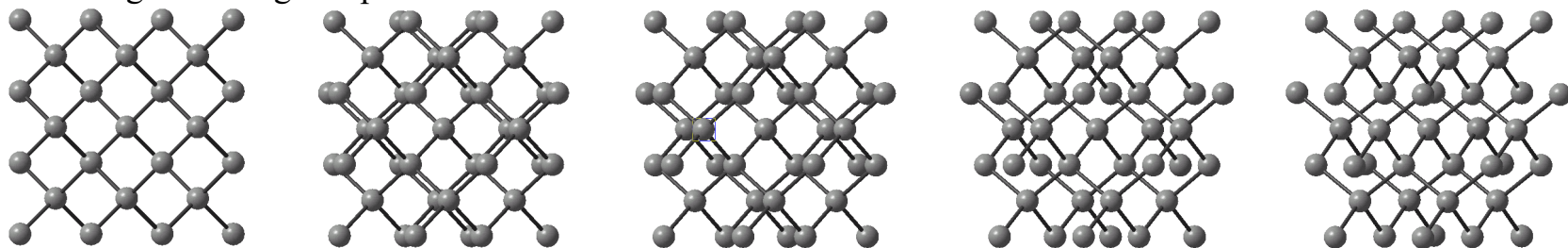
Figure 8-7 Evolution of a Gaussian profile after annealing. The Gaussian preserves its shape as it diffuses in an infinite medium.

$$\sigma'_p \Rightarrow \sqrt{\sigma_p^2 + 2Dt}$$

Ion Implantation

Channeling of Ions

Along certain crystal directions, “tubular holes” exist that allow ions to travel long distances without undergoing a high angle collision. The ions “skip” down these tubes undergoing only glancing collisions. This extends the effective range resulting in a positive skewness.



<001> with increasing angle (→) toward <100>

Critical Angle: defined as the maximum angle between the ion and the channel for a glancing collision to occur.

$$\varphi_1 = 9.73^\circ \sqrt{\frac{Z_1 Z_2}{Ed}}$$

Where Z_1 is the incident ion atomic number, Z_2 is the target atom atomic number, E is the acceleration energy in keV (voltage) and d is the atomic spacing in the direction of the ion path in angstroms. Note: Channeling is more likely for heavy ions and lower energies.

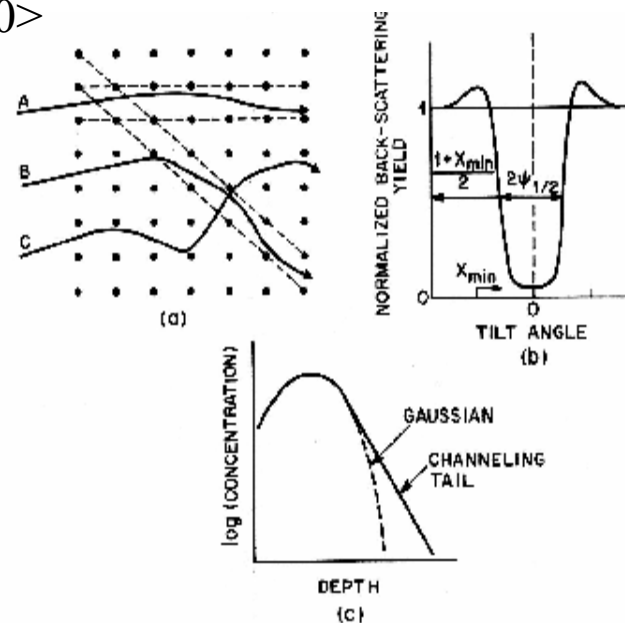


FIGURE 13 Schematic views of channeling. (a) Ion paths through a cubic lattice, showing channeled and nonchanneled cases. (b) Back-scattering yield around a channeling direction. Yield is a minimum when beam is well aligned with a channel. (c) The effect of channeling is to add a tail to the atom distribution.

Ion Implantation

Ion channeling is very sensitive to angle. Thus, for highly reproducible results, channeling needs to be avoided. Most implants are done at 7.4 degree angles (on the $\langle 763 \rangle$ plane) to minimize the channeling effect.

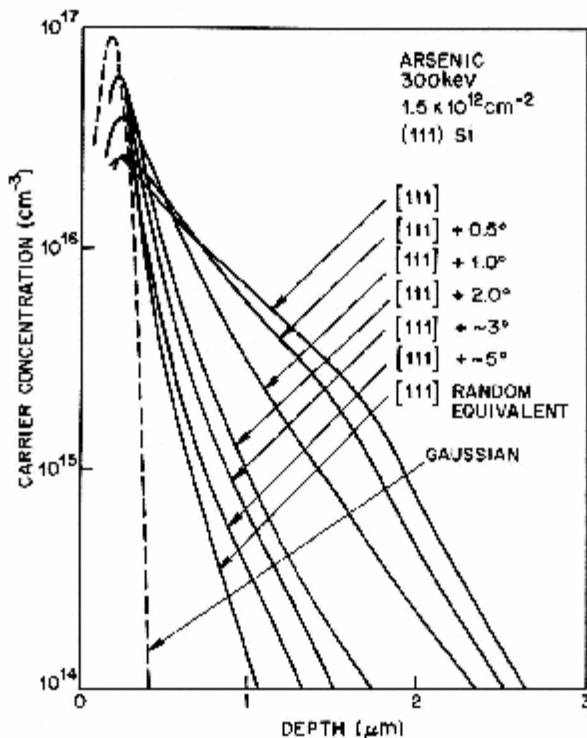


FIGURE 15

Electrically active arsenic distribution as a function of beam angle, tilted at 18° to the (110) plane. The "random equivalent" case is the usual 7° tilt used to avoid channeling, and still shows significant differences from a Gaussian. (After Wilson *et al.*, Ref. 32.)

Ion Implantation

Lateral Distribution

The lateral distribution is less precisely characterized. It is usually approximated as a simple Gaussian.

The profile from a single point (see Monte Carlo distribution) is described as,

$$n(x, y) = \frac{n_{\text{vertical}}(x)}{\sigma_{\perp} \sqrt{2\pi}} e^{-\frac{y^2}{2\sigma_{\perp}^2}} \quad \text{where } n_{\text{vertical}}(x) \text{ is a sheet concentration } [\#/cm^2]$$

For a square mask of side length $2a$ ($y=-a$ to $y=+a$), results in,

$$n(x, y) = \int_{-a}^{+a} n(x, y-l) dl = \frac{n_{\text{vertical}}(x)}{2} \left[\operatorname{erfc}\left(\frac{y-a}{\sqrt{2}\sigma_{\perp}}\right) - \operatorname{erfc}\left(\frac{y+a}{\sqrt{2}\sigma_{\perp}}\right) \right]$$

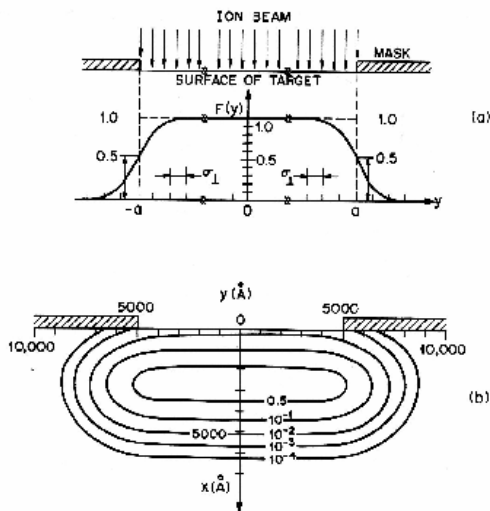


FIGURE 8
Two-dimensional implantation profiles. (a) Fraction of total dose as a function of lateral position for an opaque mask. (b) Equi-concentration contours for a 70 keV boron implant through a $1 \mu\text{m}$ slit. (After Furukawa, Matsumura, and Ishiwara, Ref. 17.)

Ion Implantation

Damage

Only nuclear stopping damages the crystal. Initially, stopping is mostly electronic resulting in little damage. As the ion is decelerated, nuclear stopping becomes more important and damage begins to occur. Thus, the maximum damage roughly corresponds with the ion range, R_p . The damage increases with the dose (more ions produce more damage).

$^{28}\text{Si} \rightarrow \text{Si}$ 300 keV 300° K

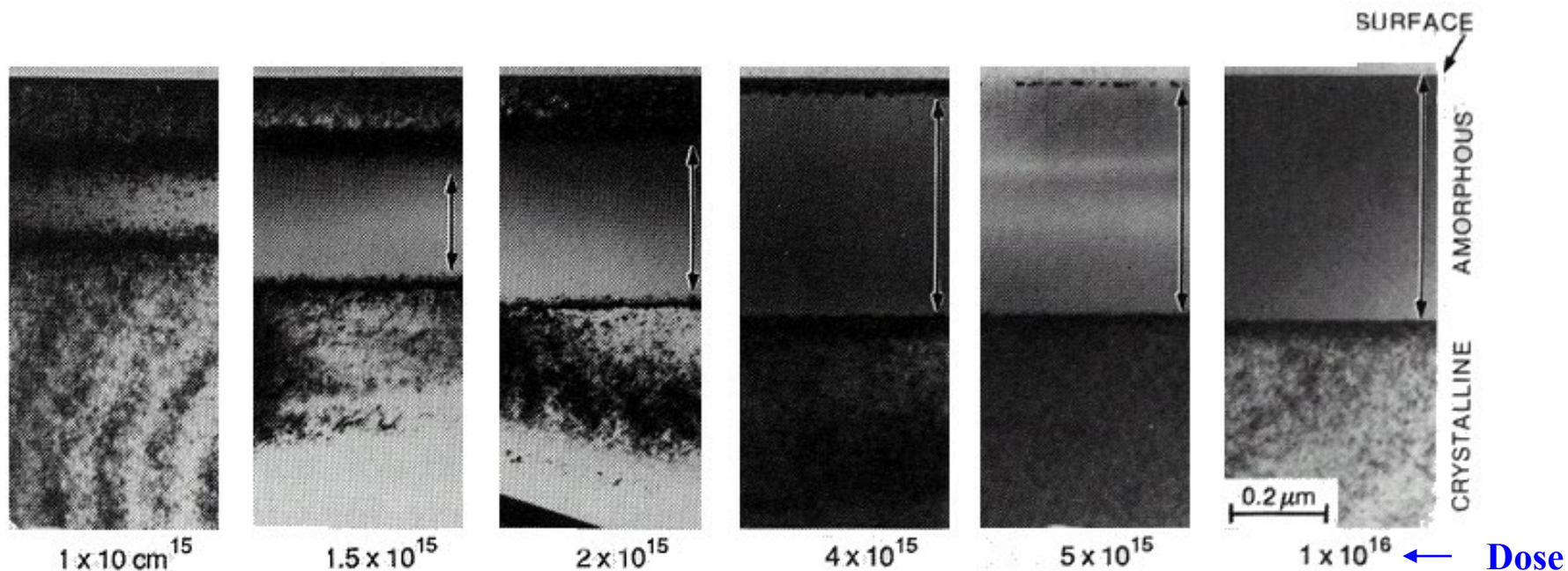


FIGURE 10

Transmission electron micrographs showing damage accumulation for silicon self-implantation as a function of dose. (After Maszara and Rozgonyi, Ref. 22.)

Ion Implantation

The maximum dose required to create amorphous material is called the *critical dose*. Because the material can anneal out damage during the implant, the critical dose increases with increasing temperature.

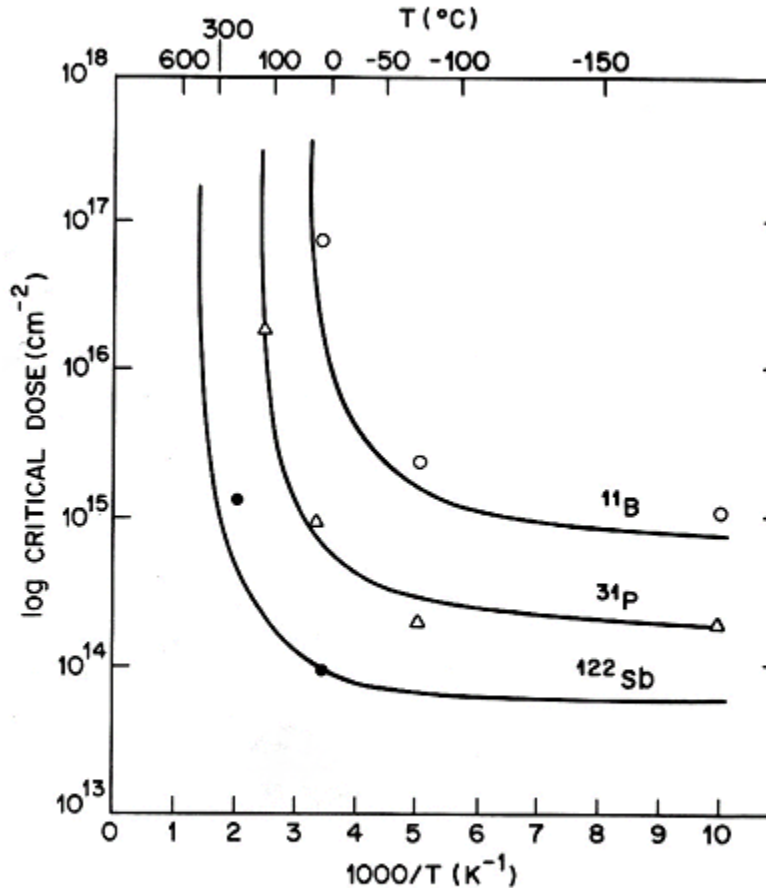


FIGURE 12

A plot of the critical dose necessary to make a continuous amorphous layer as a function of temperature. (After Morehead and Crowder, Ref. 23.)

Ion Implantation

Dopant Activation and Damage Removal

Only the substitutional impurities are “active” as dopants (supplying electrons and holes), not all implanted impurities. High temperature anneals improve the activation percentage.

For Si only, due to the high activation energies required to annihilate defects (~5 eV), it is often easier to regrow the crystal from an amorphous layer via a process known as solid phase epitaxy (activation energy ~2.3 eV in Silicon) than it is to anneal out defects. Thus, two schemes for implants are used:

- 1.) Implant above the critical dose and use low temperature anneal to regrow material
- 2.) Implant below the critical dose and use high temperature anneal to get rid of defects

Dopants can diffuse during high temperature anneal (activation energy ~3-4eV)

=====> Rapid thermal Processing (RTP) or Rapid Thermal Anneal (RTA)

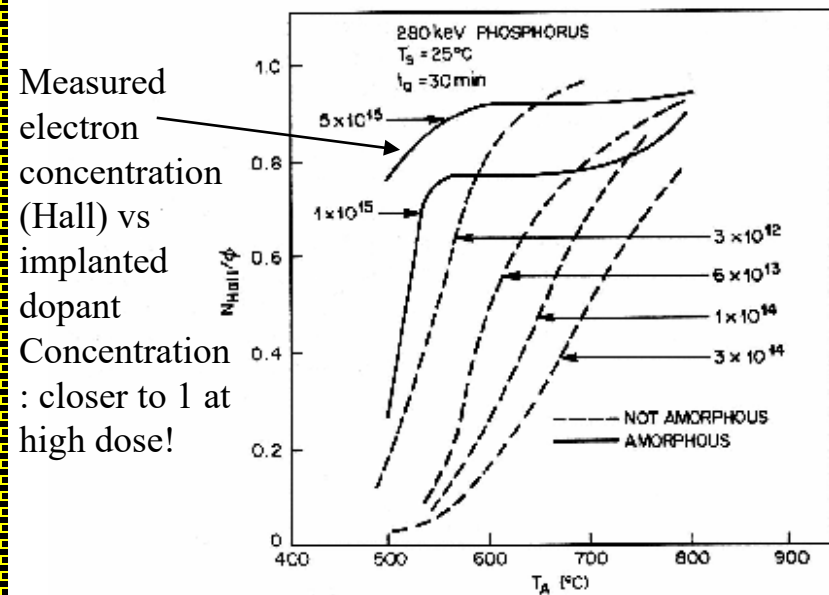


FIGURE 26 Isochronal annealing of phosphorus. The fraction of activated dopant is plotted against anneal temperature for different implant doses. Dashed lines are for partially damaging implants, solid lines for amorphizing implants. (After Crowder and Morehead, Ref. 43.)

Big difference in electrical activation

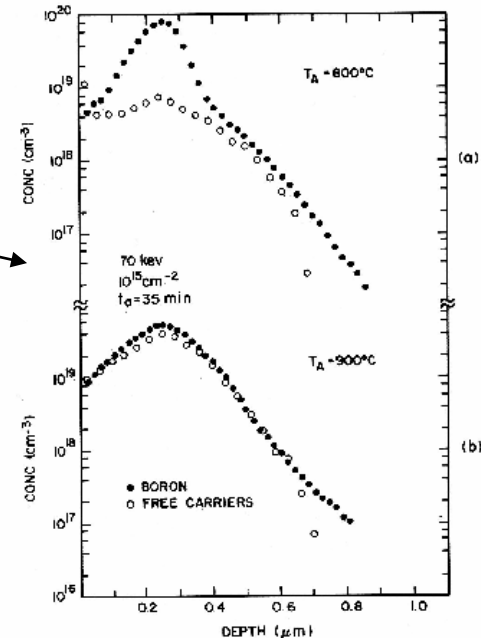


FIGURE 24 Concentration profiles of boron atoms (SIMS—solid circles) and corresponding free carrier concentrations (Hall data—open circles). (After Hojfer et al., Ref. 11.)

Ion Implantation

Other Important Issues

Intermixing

Masking materials can be “knocked” into the wafer creating unwanted impurities, or even destroying the quality of the interface.

Shadowing

The mask material needs to be very shallow to prevent shadowing effects. Thus, for small geometry devices, very dense mask materials must be used (to minimize the range) \implies C60 containing polymers (photoresist) have been employed, as well as refractory metal masks (W-tungsten).

Shallow junctions

Molecular sources instead of atomic ones: Example: $\text{BF}_2 \rightarrow \text{B} + \text{F} + \text{F}$ with the Boron energy E_B found by:

$$E_B = E_{\text{BF}_2} \left(\frac{M_B}{M_{\text{BF}_2}} \right)$$

Where the “M’s” are masses and the “E’s” are energies.

Glancing Angle Implants: shallow penetration but enhances shadowing effects.

Low Energy Implant Machines (possible but more expensive and less stable requiring more “fine tuning”).

Implantation through masks.